Food Microbiology 133 (2026) 104896

Contents lists available at ScienceDirect

Food Microbiology

journal homepage: www.elsevier.com/locate/fm

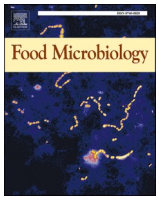

Differential phenolic metabolite and ROS responses in lettuce following infiltration with *Salmonella* and *Escherichia coli* O157:H7 accompanied bacterial log reductions

Claire L. Hudson [a], Shirley A. Micallef [a,b,*]

[a] Department of Plant Science and Landscape Architecture, University of Maryland, College Park, MD, USA
[b] Centre for Food Safety and Security Systems, University of Maryland, College Park, MD, USA

ARTICLE INFO

Keywords:
Plant secondary metabolites
Flavonoids
Biotic stress
ROS response
Food safety
Lettuce apoplast
Phenolics spectrophotometry
Human pathogens on plants

ABSTRACT

While lettuce immune responses to enteropathogens have been studied at the molecular and physiological levels, plant secondary metabolite responses have received little attention. We evaluated romaine lettuce phenolic metabolite responses to *Escherichia coli* O157:H7 and *Salmonella enterica* Enteritidis infiltrated into the leaf apoplast. Evaluating spectrophotometric profiles of leaf extracts, we detected shifts in overall phenolics and developed a semi-quantitative method to measure representative phenolics absorbing maximally at 255, 273, 280 and 329 nm, based on known standards for quercetin, gallic acid, catechin and chlorogenic acid, respectively. We also measured reactive oxygen species (ROS) accumulation and bacterial counts following enteropathogen infiltration in pre- and post-harvest leaves. Live and heat-killed *Salmonella* elicited phenolics 4 h post-inoculation (hpi) ($p < 0.05$) which declined or returned to control levels 24 hpi, while exhibiting a lag time in ROS production. Phenolics in leaves inoculated with live or heat-killed *E. coli* O157:H7 remained mostly unchanged relative to controls, while ROS was detected at both timepoints. *Salmonella* populations declined by 2 log at 4 hpi and *E. coli* O157:H7 by 1.2 log. Post-harvest leaves had a lower phenolic content than pre-harvest leaves and exhibited lower log reductions ($p < 0.05$). The spectrophotometric method proved to be a useful and efficient tool to elucidate lettuce phenolic shifts in response to enteropathogens, indicating pathogen-specific responses influenced by lettuce harvest state. This research demonstrates that the complex plant responses to enteropathogens involve plant secondary metabolite shifts that intersect with basal plant immunity, suggesting direct and/or indirect links to enterobacterial population decline in the apoplast.

Abbreviation list

CE	catechin equivalent
CGAE	chlorogenic acid equivalent
DAB	3,3′-diaminobenzidine
GAE	gallic acid equivalent
hpi	hours post-inoculation
MAMP	microbe associated molecular patterns
PAMP	pathogen associated molecular patterns
PSM	plant secondary/specialized metabolites
PTI	PAMP-Triggered Immunity
QE	quercetin equivalent
rif	rifampicin
ROS	reactive oxygen species
TSA	trypticase soy agar

1. Introduction

Foodborne pathogens like *Escherichia coli* O157:H7 and *Salmonella enterica* present serious health risks associated with leafy vegetables, potentially leading to multistate outbreaks or recalls that result in severe economic and public health consequences (Ackerley et al., 2025; Chen et al., 2023). In the United States, records of confirmed *E. coli* O157:H7 outbreaks linked to leafy greens date back to at least 1998 (Ackers et al., 1998), and since then, the United States has experienced multiple outbreaks involving the same pathogen-commodity pair (Machado-Moreira et al., 2019; Rangel et al., 2005). *Salmonella* presence in leafy vegetables is also an ongoing concern, marked by numerous recalls and some outbreaks in the past decade. A recent case involved the removal of packaged baby leaf salad from distribution in five states following an

* Corresponding author. Department of Plant Science and Landscape Architecture, University of Maryland, College Park, MD, USA.
E-mail address: smicall@umd.edu (S.A. Micallef).

https://doi.org/10.1016/j.fm.2025.104896
Received 21 May 2025; Received in revised form 11 July 2025; Accepted 5 August 2025
Available online 6 August 2025

outbreak of 31 reported illnesses and four hospitalizations (FDA, 2022).

To bolster the microbial safety of leafy vegetables, recent research has sought to shed light on human enteropathogen-plant interactions. Enteric bacteria on leaves have been shown to aggregate around trichomes and stomata and exploit cut edges to infiltrate the apoplastic space and internalize into plant tissue (George and Brandl, 2021). In turn, plants recognize and exhibit defence responses, via pathogen/microbe associated molecular patterns (PAMPs/MAMPs), when they encounter bacterial pathogens (Garcia et al., 2014; Melotto et al., 2014). *Salmonella* induced the production of reactive oxygen species (ROS) and nitric oxide (NO) in tomato leaves (Ferelli et al., 2020), while *E. coli* O157:H7 triggered ROS production and stomatal closure in lettuce (Jacob and Melotto, 2020; Roy and Melotto, 2019). Both bacterial outcomes and plant responses to these pathogens can vary by plant genotype (Ding et al., 2024; Jacob and Melotto, 2020) and the persistence of apoplastic (internalized) *E. coli* O157:H7 differs in pre- and post-harvest lettuce, with higher persistence associated with post-harvest leaves (Hudson and Micallef, 2024). Taken together, these findings point to plant responses that have the potential to modulate enteric bacterial populations, especially in pre-harvest plants capable of systemic responses.

While this knowledge regarding enteropathogen-plant interactions is crucial for developing strategies to detect enteropathogen contamination and enhance plant resilience against them, many gaps in our understanding remain. One such gap pertains to plant secondary (specialized) metabolites (PSM), which are induced during plant-microbe interactions and plant immune responses to microbes (Anjali et al., 2023). Several studies have assessed PSM levels in crops from the nutritional perspective, especially phenolics and flavonoids (Cho et al., 2023; Kim et al., 2018; Lee et al., 2022), being known for their human health benefits due to their antioxidant, antimicrobial and anti-inflammatory properties (Taniguchi et al., 2023). In plants, PSM are necessary for protection against stresses, such as ultraviolet-radiation, maintaining redox homeostasis, mediation of plant-microbe interactions and plant defence, and attracting or deterring insects (Shi and Liu, 2021; Simmonds, 2003; Wang et al., 2022). While our understanding of PSM involvement with phytopathogen interactions and the specific mechanisms intersecting with plant immunity remains limited (Anjali et al., 2023), even less is known about how these metabolites affect enteric pathogens on plants. We recently reported on how lettuce and kale responses to drought stress augmented PSM levels while also exhibiting differential susceptibility to *Salmonella* association (Liu et al., 2022, 2023) pointing to a possible function for PSM in enteropathogen modulation. Added complexity in the role PSMs may play through interacting with enteropathogens in a leafy vegetable crop comes from variability between the pre- and post-harvest state, since once leafy greens are harvested, systemic responses are severed and many physiological changes begin to occur, including the rapid decrease in total phenolic compound concentrations during storage (Rickman et al., 2007).

Our understanding of how plant association with enteric pathogens affects plant metabolite profiles in pre- and post-harvest leafy vegetables is notably limited. This gap in research is significant since, while these compounds may exert antimicrobial effects on invading microbes, they are also crucial in scavenging ROS induced by PAMPs and MAMPs to maintain redox homeostasis. Understanding these complex interactions could provide insights into plant-enteropathogen associations and their potential implications for food safety and quality. Our study, therefore, aimed to assess whether phenolic compound profiles of romaine lettuce shifted in response to internalized enteric pathogens and to detect any response differences between live plants and harvested processed leaves. Leveraging the molar absorptivity of phenolic compounds in the 240–400 nm range, we developed a spectrophotometric method to accurately and rapidly measure shifts in this compound group. This method enabled us to evaluate lettuce responses to apoplastic enteric pathogen presence by identifying variations in spectral regions, allowing for the detection of patterns and shifts throughout the course of our experiments. Moreover, we evaluated how those phytochemical shifts coincided with ROS accumulation and enteric pathogen population levels inside lettuce leaves.

2. Materials and methods

2.1. Lettuce growth conditions and processing

Seeds of romaine lettuce cultivar 'Carlsbad' (Johnny's Seeds, Waterville, ME) were sown in 5 × 5 cm pots filled with Sungro Horticulture Professional Growing Mix (Sungro Horticulture, SC). The plants were grown for 4 weeks under LED grow lights at an intensity of 405 μmol m^{-2} s^{-1}, with a 16-h photoperiod, maintained at 21 °C during the day and 16 °C overnight at 65 % relative humidity. Weekly fertilization was provided with a 100 ppm solution of Jack's 20-20-20 (Allentown, PA) after germination.

For post-harvest leaves, four-week-old romaine lettuce 'Carlsbad' leaves were harvested and washed with the commercially available sanitizer, SaniDate 15.0 (BioSafe Systems, Connecticut) at a final concentration of 175 ppm of peroxyacetic acid (PAA) and 117 ppm of H_2O_2, as per manufacturer's instructions. Leaves were cut from the plant using sterile scissors, excluding cotyledons and damaged leaves, shaken in the sanitizer solution at 100 rpm for 45 s, then transferred to a sterile stainless-steel colander to drain and air dry. Once dry, they were placed in a sterile Whirl-Pak bag (Nasco Sampling, WI USA) and stored at 4 °C for 1 week prior to the start of the experiment, to simulate a harvested, processed product kept at refrigerated temperatures.

2.2. Inoculum preparation, application, incubation and enumeration

Escherichia coli O157:H7 strain 2705C, associated with a romaine lettuce outbreak (U.S. Food and Drug Administration, 2020) and *Salmonella enterica* serovar Enteritidis strain 576710-2, an environmental strain from a feed mill, were used in this study. Both strains were adapted to rifampicin (rif) (MilliporeSigma, MA, USA). Bacteria were revived from frozen stock by streaking onto Trypticase Soy Agar (TSA, BD) plates supplemented with 50 μg mL^{-1} rif (TSA^{rif}) and incubating for 18–20 h at 35 °C. Single colonies from the overnight growth were then streaked onto fresh TSA^{rif} plates and incubated for an additional 18 h at 35 °C. The live inoculum (Live) was prepared by suspending fresh bacterial colonies in 10 mL of sterile deionized (DI) water and adjusting the suspension to a 0.5 McFarland standard using a Sensititre Nephelometer (Intertek, Integrated Technologies). Heat-killed cells (Dead) were prepared by transferring 5 mL of the live inoculum into a sterile tube, boiling in a water bath for 20 min, then cooling on ice before application to leaves. Non-viability of heat-killed cells was verified by incubation on TSA^{rif}.

On the day of the experiment, 4-week-old 'Carlsbad' lettuce plants (pre-harvest) were moved to a Biosafety Cabinet (BSC) and allowed to acclimate for 1–2 h. Using a needleless syringe, 100 μL of either the Live (7 log CFU/leaf) or Dead inoculum, or DI water (mock treatment to serve as control) were infiltrated into the abaxial surface of each of three leaves per plant. The plants were then incubated at room temperature inside the BSC, with the sash lowered and the blower turned off, for either 4 h or 24 h. For post-harvest treatments, 'Carlsbad' leaves were removed from storage bags, transferred in triplicate to new bags, inoculated as described above and incubated for 24 h. The 4 h timepoint was omitted since plant systemic responses are not possible in post-harvest leaves.

After each incubation period, leaves were carefully removed from the plant using a sterile razor blade, or from post-harvest bags using sterile forceps. In each triplet leaf set, one leaf was immediately flash-frozen in liquid nitrogen and then lyophilized for further analysis, another set aside for H_2O_2 detection as described below, and the remaining leaf used for pathogen retrieval and quantification as

previously described (Hudson and Micallef, 2024). Briefly, leaves were homogenized in 1 mL 0.1 % peptone water using a porcelain pestle by crushing the leaf through the bag. The homogenate was serially diluted and plated in duplicate on TSA^{rif} agar. The lower limit of detection was 1.7 log CFU mL^{-1}.

2.3. Preparation of leaf tissue extracts

Lyophilized leaf tissue was ground into a fine powder. A 10 mg aliquot of the powder was weighed into a 2 mL centrifuge tube and 1.5 mL of 70 % methanol (Sigma-Aldrich, MO, USA) with 0.5 % formic acid (Avantor, Inc., Radnor, PA, USA) was added. The tubes were vortexed at maximum speed for 5 min at room temperature, then extracted in the dark using a sonicating water bath (Branson 8510R-DTH, Branson Ultrasonics Corporation, CT, USA), set to 30 °C for 60 min. The extracts were filtered through a 0.45 μm nylon syringe filter (Avantor, Inc. Radnor PA, USA) and used immediately.

2.4. Development of spectrophotometric phenolic profiling and quantification method

Phenolic compounds (such as gallic and chlorogenic acid) absorb UV light maximally at specific wavelengths in the range of 240–400 nm. Some flavonoids, such as quercetin, have distinct spectra with two peaks in the region of 240–295 nm (band II, associated with ring A) and wavelengths greater than 300 nm (band I, associated with ring B, while other flavonoids such as catechin, absorb maximally at a single wavelength <300 nm (Taniguchi et al., 2023). To obtain extract profiles of plant tissue, 1.5 mL aliquot of the filtered extracts were transferred to quartz cuvettes (1 cm) for same day relative absorbance measurements using a GENESYS™ 180 UV–Vis Spectrophotometer (ThermoFisher Scientific), scanning from 240 to 400 nm at 1 nm intervals. We then developed a phenolic metabolite quantification method using these UV–vis spectral scans. Extract profiles were analysed for phenolic compound equivalents for quercetin (QE_{255}), gallic acid (GAE_{273}), (+)-catechin (CE_{280}) and chlorogenic acid ($CGAE_{329}$) (Avantor, Inc. Radnor PA, USA) were determined using calibration curves produced from 1 mg mL^{-1} standards for each metabolite at λ_{max} 255, 273, 280 and 329 nm, respectively. Dilutions of extracts were made as needed to keep relative absorbances within the standard curve absorbance range. Using the linear equation generated from the regression model for each metabolite, we used the following formula to determine the equivalent concentration g^{-1} dry tissue:

$$\frac{(C \times V \times DF)}{W}$$

Where C = concentration from standard curve in mg mL^{-1}, V = volume in mL, DF = Dilution factor and W = weight of dry tissue extracted in g.

2.5. Histochemical detection of H_2O_2 in pre-harvest leaves

The amount of H_2O_2 in leaves in response to mock (DI water) or Live and Dead pathogen inoculation by syringe infiltration was detected using the 3,3′-diaminobenzidine (DAB) staining method, as described by Ferelli et al. (2020). Post-inoculation, the leaves were collected and submerged in 10 mL of DAB solution made of 1 mg mL^{-1} aqueous DAB (Alfa Aesar, Ward Hill, MA, USA), 200 mM Na_2HPO_4 (VWR, West Chester, PA, USA), 0.05 % Tween 20 (Amresco, Solon, OH, USA), with pH adjusted to 7 using ~100 μL of 1 M NaOH. The leaves were incubated overnight in the dark. The following day, leaves were decolourised by boiling in absolute ethanol for at least 20 min, transferred to glycerol-soaked paper towels, and once pliable, gently dabbed dry with Kim wipes and placed in clear plastic sleeves for imaging. The leaves were scanned at 600 dots per inch (dpi) using a Sharp MX-M365 printer scanner (Montvale, NJ, USA). Images were analysed on a transparent background using Adobe Photoshop 25.5.1. Percent leaf area DAB stained was calculated by obtaining the total leaf area (pixels) and the total stained area (pixels). Using the histogram function, total pixel counts per leaf were measured. Then, utilizing the colour range tool and eyedropper selector, pixels with brown staining (indicative of H_2O_2 production) were selected and recorded. Leaf area stained was calculated as a percentage of total leaf area.

2.6. Statistical analysis

Experiments were repeated at least three time with at least four biological replicates per experiment and the data were pooled for analysis. At least one of the experiments included DAB staining at two time points for pre-harvest leaves. Bacterial counts were taken in duplicate, averaged and log-transformed to obtain log CFU/leaf measurements. To account for the small differences in inoculum concentration across multiple experiments, the log reduction from the inoculum was calculated. Metabolite equivalents and DAB stain were represented as values relative to mock-inoculated leaves. To meet the assumptions for parametric statistical analysis of % DAB area stained, data were square-root transformed prior to analysis.

Data were analysed using JMP Pro ver. 17.0 (SAS Institute Inc., Cary, NC). The least squares mean model with Tukey's Honestly Significant Difference (HSD) test was employed to assess differences in metabolite equivalent concentrations and DAB stain area relative to mock treatment levels, as influenced by incubation time (4 or 24 h) and pathogen state (Live or Dead). ANOVA analysis with the Dunnett's Method for multiple comparisons was employed to test for differences between mock-treated (control) and Live or Dead inoculated leaves for each dependent variable grouped by pathogen strain and incubation time.

3. Results

3.1. Development of spectrophotometric phenolic profiling and quantification method based on standards with peak absorbances at varying wavelengths

To profile and quantify phenolics in lettuce leaf extracts, we developed a method that calculates metabolite equivalents from UV–vis scans of lettuce extracts. The phenolic acids, gallic and chlorogenic acid, and the flavonoids, catechin and quercetin, were selected as standards for having peak absorbances in the two main bands typical of phenolics (Table 1, Fig. 1). The presence of these compounds has been confirmed in romaine lettuce extracts via chromatography and mass spectrometry (Ji et al., 2015). Utilizing scan mode between 240 and 400 nm, we obtained spectra for the serially diluted standards and determined the wavelength for the strongest peak (λ_{max}) that remained stable and displayed no drift across the serial dilutions. To construct the standard curves, we used a linear regression model to relate the known concentrations of the standard to the measured absorbance at each specific λ_{max}. The fitted models were evaluated using several fit diagnostics to assess accuracy and reliability (Table 1). Each model generated R^2 values ranging from 0.981 (catechin) to 0.999 (gallic acid, quercetin and chlorogenic acid) and robust and statistically significant F-ratios, indicating that each linear model was a highly significant fit for our standards (Table 1).

3.2. Secondary metabolite equivalent concentrations in romaine lettuce were affected by harvest stage

Romaine lettuce 'Carlsbad' plants were grown, harvested and processed in-house, enabling a direct comparison of UV–Vis spectral profiles between pre- and post-harvest conditions of the same cultivar grown under the same conditions. The overall UV–Vis profile obtained from extracts of uninoculated leaves revealed marked differences between pre- and post-harvest stages (Fig. 1). The profiles of pre-harvest

Table 1
Fit diagnostics for phenolic compound standard curves generated at specific λ_{max} for each metabolite.

Metabolite	$\lambda_{max\ (nm)}$	Linear equation ($y = mx + b$)	R^2	Sum of Squares Regression (SSR)	Residual Sum of Squares (RSS)	*F*-ratio	*p*-value
Quercetin	255	Abs $= 68.186x + 0.010$	0.999	7.415	0.0002	104254.3	<0.0001
Gallic acid	273	Abs $= 60.532x + 0.017$	0.999	5.423	0.0013	16707.6	<0.0001
Catechin	280	Abs $= 9.814x + 0.171$	0.981	5.116	0.0098	156.2	0.001
Chlorogenic acid	329	Abs $= 56.271x + 0.063$	0.999	3.166	0.0033	2904.7	<0.0001

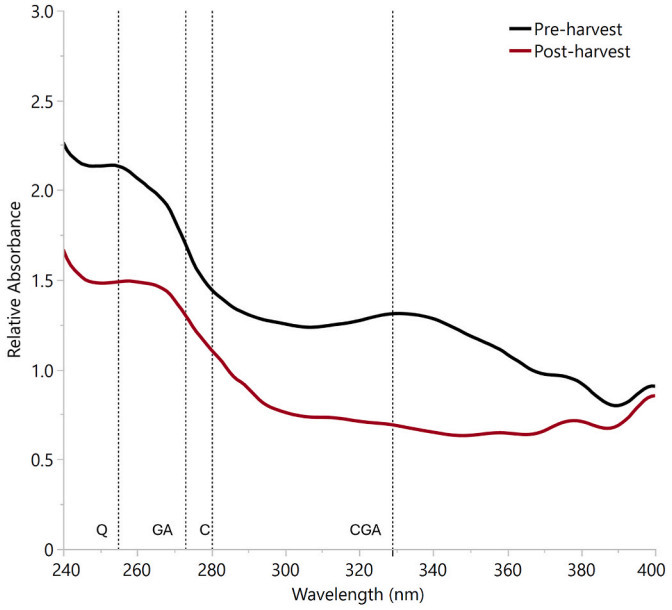

Fig. 1. UV–Vis spectral scans of crude extracts of pre-harvest and post-harvest leaves of romaine lettuce 'Carlsbad'. Dashed lines represent wavelengths at which absorbances were measured for metabolite equivalent calculations (Q: Quercetin 255 nm, GA: Gallic Acid 273 nm, C: Catechin, 280 nm, CGA: Chlorogenic Acid 329 nm).

leaves indicated higher metabolite concentrations compared to post-harvest leaves. Overall, QE_{255} equivalent levels were the highest and $CGAE_{329}$ levels the lowest in pre-harvest leaves. On average, CE_{280} and $CGAE_{329}$ showed a considerable decrease post-harvest, with a reduction of 2.2 and 1.3 mg equivalent/g dry tissue (mgE g^{-1}), respectively, compared to pre-harvest leaves (CE_{280}, $p < 0.05$; $CGAE_{329}$, $p < 0.001$) (Fig. 1). GAE_{273} and QE_{255} were also lower in post-harvest leaves, decreasing by 0.5 mgE g^{-1} ($p = 0.01$) and 0.8 mgE g^{-1} ($p < 0.001$), respectively (Fig. 1).

3.3. Phenolic levels in pre-harvest romaine lettuce leaves changed in response to internalized Live and Dead enteric pathogens in a pathogen specific manner

The UV–vis profiles of pre-harvest lettuce leaf extracts at 4 and 24 h post-inoculation (hpi) (Fig. 2) and post-harvest leaves 24 hpi (data not shown) were generated to assess the impact of Live or Dead *E. coli* O157:H7 and *Salmonella* Enteritidis on plant phenolic levels. Phenolic equivalent concentrations for these compounds in pathogen-inoculated samples were calculated relative to mock-inoculated leaves, provided in Table 2. We observed differential responses to the two pathogens and between incubation times in pre-harvest leaves (Fig. 3).

Pre-harvest leaves inoculated with *E. coli* O157:H7 showed a weak response to the introduction of the pathogen into the apoplast. After 4 hpi, all four metabolites in pre-harvest leaves inoculated with either Live or Dead *E. coli* O157:H7 remained unchanged compared to the mock-treated leaves (Fig. 2A and 3A). At 24 hpi with live bacteria, we detected a downward shift in relative absorbance of leaf extracts between 280 and 380 nm (Fig. 2B) and reductions in CE_{280} by 2.9 ± 1.4 mgE g^{-1} and $CGAE_{329}$ by 1.0 ± 0.5 mgE g^{-1} relative to mock-inoculated levels but these changes were not statistically significantly supported (Fig. 3A).

In contrast, pre-harvest leaves inoculated with *Salmonella* Enteritidis showed a stronger response (Fig. 2C, D, 3B). Notably, all four metabolite equivalents were elicited 4 hpi when leaves were infiltrated with either Live or Dead *Salmonella* (Fig. 2C and 3B). The highest increases were observed in CE_{280}, which were 5.3 ± 1.4 and 5.1 ± 1.4 mgE g^{-1} higher than the controls on leaves infiltrated with Live and Dead *Salmonella*, respectively ($p < 0.05$ for both; Fig. 3B). $CGAE_{329}$ increased by 1.8 ± 0.6 and 2.0 ± 0.6 mgE g^{-1} compared to the controls in Live ($p = 0.06$) and Dead ($p < 0.05$) inoculated leaves, respectively, and GAE_{273} rose by 0.7 ± 0.2 and 0.6 ± 0.2 mgE g^{-1} in Live ($p < 0.05$) and Dead ($p = 0.07$) inoculated leaves relative to the mock-treated leaves, respectively. Additionally, QE_{255} increased 4 h post Live-inoculations by 0.9 ± 0.2 mgE g^{-1} ($p < 0.05$) and leaves inoculated with Dead *Salmonella* increased by 0.8 ± 0.2 mgE g^{-1} ($p = 0.06$) (Fig. 3B).

The metabolite induction observed at 4 h was reversed 24 hpi. With Live *Salmonella* infiltration, all metabolite equivalent concentrations dropped to levels below those measured for mock-inoculated leaves, although the differences from mock-treated leaves were small ($p \leq 0.1$ for all) (Fig. 2D and 3B). With Dead *Salmonella*, GAE_{273} and QE_{255} remained lower than mock-inoculated leaves 24 hpi ($p < 0.05$ for both), while CE_{280} ($p = 0.06$) and $CGAE_{329}$ ($p = 0.08$) were slightly lower, respectively (Fig. 3B). Moreover, all metabolite equivalent levels measured at 4 hpi differed from levels measured at 24 hpi (CE_{280}, GAE_{273}, QE_{255}, $p < 0.01$; $CGAE_{329}$, $p < 0.05$), regardless of whether pathogen was viable or heat-killed.

Post-harvest leaves showed no differences in phenolic levels compared to the mock-treated leaves when inoculated with Live or Dead *E. coli* O157:H7 or *Salmonella* (data not shown).

3.4. Greater log reductions of E. coli O157:H7 and Salmonella Enteritidis in the pre-harvest stage

Log reductions of either pathogen on pre-harvest leaves were comparable at both incubation times of 4 and 24 hpi. However, Live *E. coli* O157:H7 infiltrated into leaves in the pre-harvest state and incubated for 4 hpi showed greater declines ($p < 0.05$) compared to populations in post-harvest leaves 24 hpi, with reductions relative to inoculum of 1.2 and 0.6 log, respectively (Fig. 4A). When infiltrated with *Salmonella*, leaves in the pre-harvest state yielded lower counts at both 4 and 24 hpi, compared to post-harvest leaves (Fig. 4B). Pre-harvest declines were calculated at 2.2 and 2.0 log, respectively ($p < 0.001$ for both time points), while post-harvest leaves 24 hpi exhibited a smaller reduction of 1.3 log relative to inoculum.

3.5. H_2O_2 detection in pre-harvest leaves

The production of H_2O_2 in leaves at the site of infiltration with Live *E. coli* O157:H7 was evident 4 hpi and showed markedly more staining compared to mock-inoculated leaves (9.5 % ± 2.5, $p < 0.01$). In contrast, leaves inoculated with Live *Salmonella* Enteritidis did not show increased DAB stain compared to mock-inoculated leaves 4 hpi

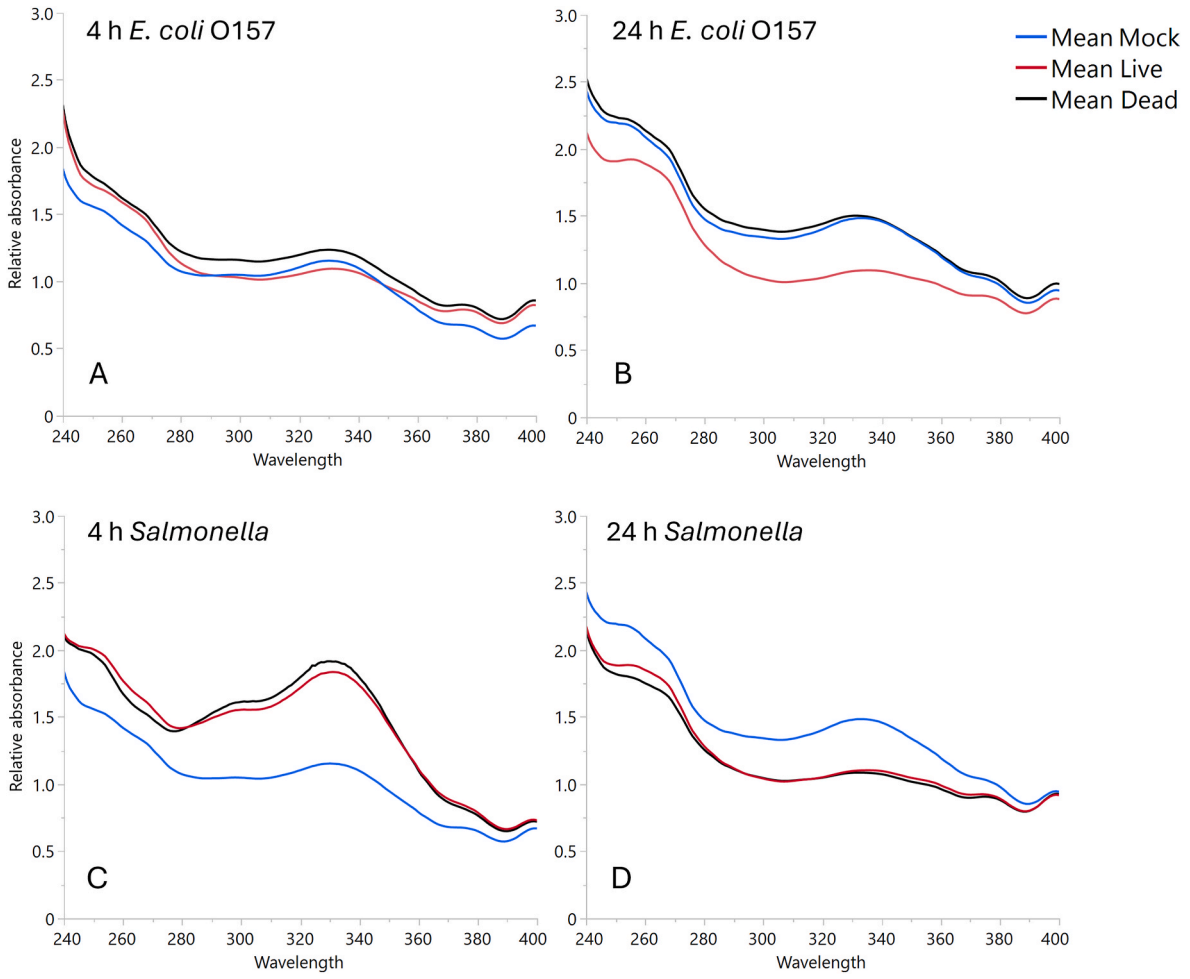

Fig. 2. UV–vis spectral scans of pre-harvest lettuce 'Carlsbad' leaf extracts following inoculations with *E. coli* O157:H7 at 4 h (A) and 24 h (B), and with *Salmonella* Enteritidis at 4 h (C) and 24 h (D).

Table 2
Metabolite equivalent (mgE g^{-1} dry weight) in pre- and post-harvest 'Carlsbad' leaves mock-inoculated with deionized water.

Metabolite	Equivalent concentration mgE g^{-1} dry tissue		
	Pre-harvest		Post-harvest
	4 h	24 h	24 h
Catechin	13.80	19.95	15.68
Gallic acid	2.90	4.21	3.41
Quercetin	3.30	4.76	3.47
Chlorogenic acid	2.90	3.77	1.86

(Fig. 5A). After 24 h, DAB stain remained higher in Live *E. coli* O157:H7 inoculated leaves (8.9 % ± 4.3, $p = 0.05$) compared to controls and at this time we saw a strong response from leaves inoculated with Live *Salmonella enterica* Enteritidis (13.7 % ± 5.1, $p = 0.01$) (Fig. 5A and B). Dead *E. coli* O157:H7 induced a low level of H_2O_2 which was not significantly altered from mock-treated leaves. Of note, the variability in these measurements was quite high, resulting in no significant differences by Live/Dead pathogen state nor hpi. By contrast, H_2O_2 accumulation in Live *Salmonella* inoculated leaves 24 hpi was markedly higher than 4 hpi and in leaves receiving Dead *Salmonella* ($p < 0.05$; Fig. 5A and 4B). A multiple regression model to evaluate the effect of pathogen species, pathogen state and incubation time on the ROS response in leaves explained 35.5 % of the variability (F-Ratio 4.41, $p < 0.01$). The strongest effects identified were incubation time ($p < 0.01$) driven by the *Salmonella* response (Fig. 5) and pathogen state (live or heat-killed) ($p < 0.05$). Overall, pathogen species was not found to be a significant factor.

4. Discussion

Enteric pathogen-plant associations have been shown to invoke reciprocal genetic and physiological responses, resulting in the expression of plant defence and bacterial tolerance mechanisms. This study addresses a knowledge gap relating to the *in planta* secondary metabolite response to enteric pathogens. Overall, we found that lettuce phenolic content shifted in response to enteric pathogens delivered to the apoplast of romaine lettuce leaves, as related to the representative compounds catechin, chlorogenic acid, gallic acid and quercetin. Whether phenolic metabolites increased or decreased was dependent on enteric pathogen species and the harvest state of inoculated leaves. *Salmonella* elicited phenolics at 4 h in pre-harvest plants, unlike *E. coli* O157:H7 which provoked no such phenolic shift. One day later, both pathogens caused an attenuation of phenolic levels. The viability of the pathogen was discriminant only in the *E. coli* O157:H7 response, while both live or heat-killed *Salmonella* induced a decline in lettuce phenolics. Concomitantly, pathogen population declines were greater and ROS onset was delayed in leaves inoculated with *Salmonella* compared to *E. coli* O157:H7, suggesting that the magnitude and timing of the plant response is pathogen specific and may modulate bacterial persistence.

It has long been established that the initial ROS burst, in recognition of plant pathogenic bacteria at least, occurs in the apoplast (Torres et al.,

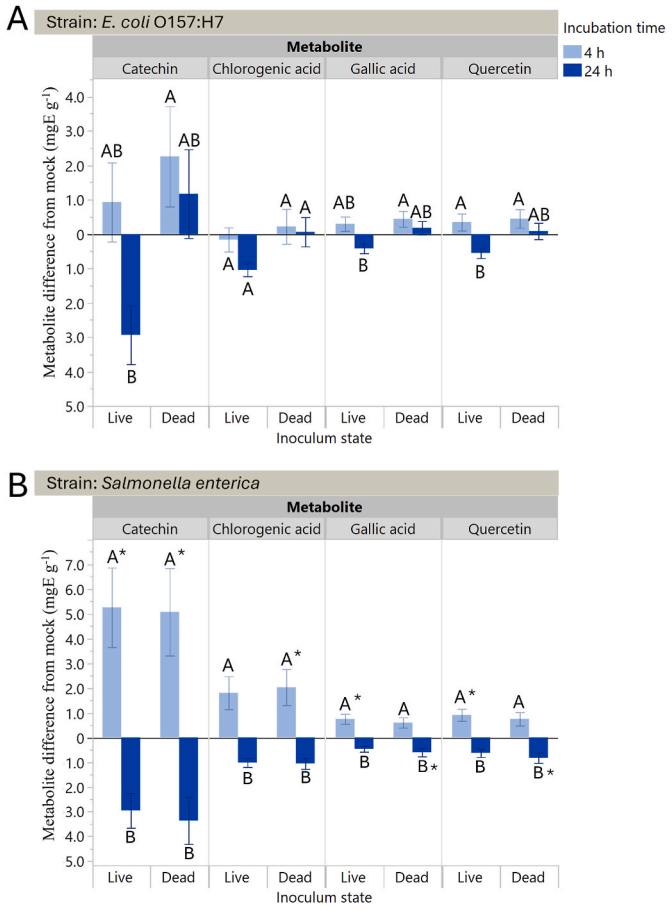

Fig. 3. Metabolite equivalent (mgE g^{-1} dry weight) of pre-harvest romaine lettuce 'Carlsbad' leaves inoculated with live or dead *E. coli* O157:H7 or *Salmonella* Enteritidis represented as difference relative to mock-inoculated leaves. Capital letters denote significant differences due to inoculum and incubation time within each metabolite (LS means ANOVA and Tukey HSD). Asterisks indicate significant differences between pathogen- and mock-inoculated leaves (ANOVA with Dunnett's test against mock; * denotes $p \leq 0.05$).

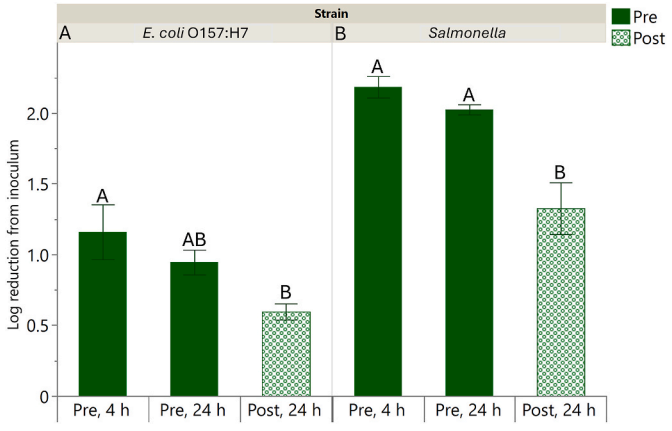

Fig. 4. *Escherichia coli* O157:H7 and *Salmonella* log reductions from inoculum ($p < 0.05$ and $p < 0.01$, respectively) 4 and 24 h post-infiltration into pre- and post-harvest romaine lettuce 'Carlsbad' leaves. Capital letters denote statistically significant differences using LS means ANOVA and Tukey HSD grouped by strain.

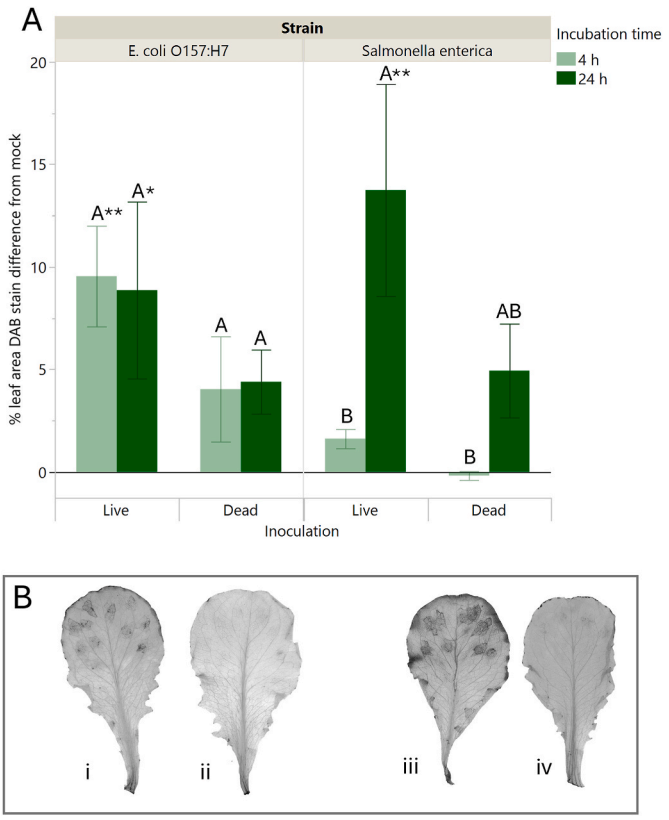

Fig. 5. (A) Percent leaf area DAB stained, expressed as difference from mock-inoculated leaves 4 and 24 hpi with live and heat-killed *E. coli* O157:H7 and *Salmonella* on pre-harvest 4-week-old romaine lettuce 'Carlsbad'. Capital letters indicate differences (LS means ANOVA and Tukey HSD $p < 0.05$) for each species separately. Asterisks indicate significant differences from mock-inoculated leaves (ANOVA with Dunnett's test, $^{**}p \leq 0.01$, $^{*}p \leq 0.05$. (B) Examples of DAB stained pre-harvest 'Carlsbad' leaves 24 hpi with i) live or ii) heat-killed *E. coli* O157:H7 and iii) live or iv) heat-killed *Salmonella*.

2006). *Salmonella* and *E. coli* O157:H7 elicit an ROS response in leaves (Ferelli et al., 2020; Jacob and Melotto, 2020), to which both pathogens respond by up-regulating ROS and NO detoxification genes (Ding et al., 2025; Han et al., 2020). Respiratory burst oxidase homologues (RBOH) are the major ROS generating enzymes in plants, activated in response to the PAMP-triggered Ca^{2+} influx into cells (Qi et al., 2017). ROS accumulation was evidenced in our study by the detection of H_2O_2 in lettuce inoculated with live *E. coli* O157:H7 and *Salmonella*. It has been suggested that another potential source of MAMP-triggered ROS could involve the pro-oxidant action of phenolic compounds (O'Brien et al., 2012). The phenolic acetosyringone, known from the tobacco apoplast, caused a high and prolonged redox potential (consistent with high ROS) in the presence of H_2O_2 and horseradish peroxidase, *in vitro* (Baker et al., 2014). In our study, the sustained H_2O_2 detection in lettuce responding to enteric pathogens 24 hpi could indicate that phenolic compounds were contributing to a sustained ROS burst, but further investigation is needed to confirm this.

Phenolic compounds are better known for their ROS scavenging activity by acting as electron donors, making them powerful antioxidants and contributing to redox homeostasis in plants. While phenolic compounds are largely confined to the intracellular compartments of plant cells, it has been shown that metabolites such as flavonoids are transported to the apoplast via vesicle trafficking when needed (Zhao and Dixon, 2010; Podgórska et al., 2017). Phenolic compounds can also be bound to cell walls or occur freely in the apoplast (Dragišić Maksimović et al., 2008; Hutzler et al., 1998). ROS detoxification capacity in the apoplast is low compared to intracellular mechanisms and

once phenolics have been quenched, ROS will continue to accumulate in the apoplastic space (Podgórska et al., 2017). We detected higher levels of H_2O_2 in *Salmonella*-inoculated leaves at 24 h. The presence of ROS could have a direct restricting effect on enteric bacteria and we did indeed measure a higher log reduction in *Salmonella* than *E. coli* O157:H7. However, this reasoning could not be extended to the 4 h timepoint, during which low H_2O_2 levels coincided with high *Salmonella* log reduction. Moreover, at least for our lettuce system, this could not be attributed to active immune response suppression by *Salmonella*, as has been suggested for other plant systems (Shirron and Yaron, 2011), since little H_2O_2 was detected in plants inoculated with heat-killed *Salmonella*. The concomitant increase in phenolic compounds measured in *Salmonella*-inoculated lettuce at this time point, however, suggests that they were induced to neutralize an oxidative environment, likely caused by an earlier strong ROS burst following *Salmonella* inoculation. In turn, this ROS burst could have caused the observed *Salmonella* log reduction and would explain the lack of H_2O_2 detected at the same time point, which would have been scavenged by the high levels of phenolics induced. Support for this scenario, whereby an inverse relationship existed between ROS and phenolic levels, comes from a study that monitored the phenolic levels and redox potential of tobacco cell suspensions to which a *Pseudomonas* pathovar was added (Baker et al., 2013). Several hours post-inoculation of the cell suspension with the phytopathogen resulted in an increase in the redox potential of the suspension (extracellular), which coincided with a decrease in antioxidant capacity (Baker et al., 2013). In addition, in our study, *Salmonella* itself could have contributed to ROS detoxification, a known *Salmonella* response to the plant niche (Goudeau et al., 2013; Han et al., 2020).

The antimicrobial action of plant phenolic compounds is well established. As such, we cannot overlook the possibility that the induced phenolic compounds detected in lettuce in response to *Salmonella* were released for their direct antimicrobial action. Numerous *in vitro* studies have shown that chlorogenic acid, gallic acid, catechin and quercetin can inhibit the growth of both *E. coli* and *Salmonella* and also restrict *E. coli* biofilm formation (Bae et al., 2022; Shao et al., 2015; Sun et al., 2020). The primary mode of action for these phenolics is generally attributed to disruption of the bacterial cell membrane, leading to increased permeability, leakage of cellular contents and lipid damage (Wang et al., 2018) which in some cases is irreversible (Borges et al., 2013). Among these phenolic compounds, quercetin is believed to interact more strongly with bacterial membranes because of its amphiphilic structure, which allows it to insert into lipid bilayers and disrupt membrane integrity (Nguyen and Bhattacharya, 2022). In our study, we expect that several unknown phenolic compounds were elicited in addition to the four metabolites we quantified. These metabolites might have dual ROS scavenging and antimicrobial action. Future research should evaluate how ROS and apoplastic phenolics, induced in response to enteric pathogens, work in balance to maintain redox homeostasis in plants, while limiting enteropathogen populations.

There is still debate regarding whether plants perceive enteric pathogens as opportunists or pathogens. While enteric bacteria rarely cause visible disease symptoms in plants, they can trigger basal plant immune responses similar to those induced by plant pathogens - specifically PAMP-Triggered Immunity (PTI), which is a broad and rapid defence activated by conserved microbial patterns such as flagellin, including Ca^{2+} and ROS signalling, stomatal closure and callose deposition between the plasma membrane and the cell wall to limit pathogen spread (Garcia et al., 2014; Meng et al., 2013; Oblessuc et al., 2020; Shirron and Yaron, 2011). Nevertheless, differences have been identified in plant responses to *E. coli* O157:H7 versus *Salmonella* (Roy et al., 2013). In our system, the lettuce ROS response was detected at the earlier timepoint against Live *E. coli* O157:H7 and sustained for 24 h, accompanied by a decline in some phenolics. This pattern is reminiscent of the response reported for a saprophyte in *in vitro* tobacco cell suspension studies, whereby an initial early spike in redox potential in the extracellular matrix stabilized at a level higher than the control, accompanied by a sharp decline in antioxidant capacity (Baker et al., 2013). By contrast, in our study, the *Salmonella* ROS spike arrived later, but was stronger and was preceded by upward shifts in phenolic compounds (and a stronger inhibition of the enteric bacterial population). This pattern matches more closely that described for the avirulent pathogen to tobacco cells (Baker et al., 2013).

In our study we detected shifts in compounds absorbing in 240–400 nm range and used specified wavelengths to obtain equivalent levels of known standards. While our study does not confirm the dynamics of specific phenolics, we detected the largest fluctuations in the equivalents for catechin and chlorogenic acid. One other study, evaluating apoplastic phenolic compound changes in tobacco plants, also identified hydroxycinnamic acid derivatives (precursor to catechin) and chlorogenic acid isomers in response to virulent and avirulent pathogens, as well as a saprophyte (Baker et al., 2015). While the patterns of apoplastic phenolic induction in tobacco plants (*Nicotiana tabacum*) were not directly comparable to what we observed in romaine lettuce, the induced compounds matched our study. This could be partly due to the fact that we were measuring both extra- and intracellular levels of phenolics. Of note, however, is that Baker et al. (2015) suggest that increased phenolic levels may have been derived from intracellular reserves. Having measured the total levels of phenolics, our study suggests *de novo* synthesis of phenolics, at least in response to *Salmonella*. Further research is needed to confirm this hypothesis.

In pre-harvest leaves, we observed elicitation of phenolic metabolites from infiltrations with both live and heat-killed *Salmonella*, with an equal phenolic compound response elicited regardless of cell viability. In contrast, phenolic levels in leaves inoculated with live or dead *E. coli* O157:H7 did not change markedly. Nevertheless, the highest phenolic equivalents in *E. coli* O157:H7 inoculated plants were obtained 4 hpi with dead inoculum, while the lowest were measured 24 hpi with live cells. Taken together, these data suggest that while a heat-stable MAMP in both *Salmonella* and *E. coli* O157:H7 is recognized by lettuce, another mechanism appeared to be at play in the case of live *E. coli* O157:H7, which may have had a slight dampening effect on the plant metabolite (but not the ROS) response.

Post-harvest leaves had lower phenolic content compared to pre-harvest leaves. The PAA-H_2O_2 sanitizer used in this study is a powerful oxidizing agent that is utilized widely for pathogen control during post-harvest rinsing of leafy greens (Stearns et al., 2022). While washing with this sanitizer may reduce the population of foodborne pathogens after a contamination event (Stearns et al., 2022), it seems plausible, given the depleted phenolic content of post-harvest leaves (observed herein), that if a contamination event were to occur post-wash, leaves may be more hospitable to enteric pathogens. In our study, post-harvest leaves exhibited lower log reductions for both enteric pathogens (*E. coli* O157:H7 < *Salmonella* Enteritidis) compared to pre-harvest leaves, which is consistent with previous work (Brandl and Amundson, 2008; Hudson and Micallef, 2024). Taken together, it seems that phenolic content and harvest state are key factors influencing the persistence of both *Salmonella* Enteritidis and *E. coli* O157:H7 in the apoplast.

The analysis of total phenolic and flavonoid content is typically carried out using colorimetric assays, such as the Folin–Ciocalteu and aluminium chloride assays, which are valuable tools for estimating total antioxidant capacity of extracts but have serious limitations (Lester et al., 2012; Shraim et al., 2021). These methods offer only a partial view of the compounds present. More advanced techniques, such as HPLC mass spectrometry with quantitative time of flight, can deliver precise measurements of specific metabolites (Otify et al., 2023), but these methods are costly and time-consuming. In our study, we focused on efficiently obtaining overall profiles of phytocompounds in sample extracts, rather than on exact quantification of unknown metabolites. To achieve this, we utilized scanning spectrophotometry to generate UV–vis profiles for each plant extract. This method provides a novel visualization tool for emerging trends throughout the experiments. We were quickly able to observe acute plant responses to Live and Dead

Salmonella Enteritidis 4 hpi in pre-harvest leaf extracts in specific regions of the spectrograph, for example the increased absorbances between 300 and 360 nm, which indicated an increase in metabolites absorbing maximally in this region, for instance $CGAE_{329}$. We were also able to quickly convert single absorbance values from a wavelength of interest to produce semi-quantitative equivalent values generated from standard curves. This method is cheap, accessible and efficient when estimating relative changes in metabolite profiles of plant extracts. However, it is important to recognize that crude extracts may contain hundreds of metabolites, some of which may have similar maximal absorbance wavelengths to the target standard compounds. Future work could adopt mass spectrometry to hone in on specific compounds of interest.

5. Conclusion

This study showed how the lettuce response to leaf-infiltrated enteric pathogens *E. coli* O157:H7 and *Salmonella enterica* involves phenolic metabolite shifts in leaves. By simultaneously measuring ROS levels in leaves, our study also evaluated the connection with plant immunity involvement. While responses varied by pathogen species, the dynamic changes in phenolic profiles detected also coincided with an ROS response. In the case of *Salmonella*, phenolic metabolite elicitation preceded an ROS burst. These effects were accompanied by *Salmonella* log reductions. By contrast, we detected unremarkable metabolite shifts with *E. coli* O157:H7, but a more consistent ROS response, coinciding with a weaker restrictive effect on the bacterial population. This study demonstrated that plant secondary metabolites can be a significant component of the plant's response to enteric pathogens. Our findings suggest that the phenolic response is complex, interconnected with the plant immune response and may play a direct or indirect role in modulating enteric bacterial populations in lettuce.

CRediT authorship contribution statement

Claire L. Hudson: Writing – original draft, Visualization, Validation, Methodology, Investigation, Formal analysis, Data curation, Conceptualization. **Shirley A. Micallef:** Writing – review & editing, Writing – original draft, Validation, Supervision, Resources, Project administration, Methodology, Funding acquisition, Formal analysis, Conceptualization.

Declaration of competing interest

The authors declare that they have no known competing financial interests or personal relationships that could have appeared to influence the work reported in this paper.

Acknowledgements

We would like to thank Dr Jean-Gilles Beaubrun for donating *Salmonella* Enteritidis used in this study.

Graphical abstract was created in BioRender. Hudson, C. (2025). https://BioRender.com/r9bioqc.

This work is supported by the Agriculture and Food Research Initiative, project award no. 2022-67017-36582, from the U.S. Department of Agriculture's National Institute of Food and Agriculture.

Data availability

Data will be made available on request.

References

Ackerley, N., Berlind, A., Black, M., Kho, K., McLaughlin, C., Sassi, A., Sertkaya, A., Walker, S., 2025. Costs of overly broad recalls. J. Food Protect. 88, 100450. https://doi.org/10.1016/j.jfp.2025.100450.

Ackers, M., Mahon, B.E., Leahy, E., Goode, B., Damrow, T., Hayes, P.S., Bibb, W.F., Rice, D.H., Barrett, T.J., Hutwagner, L., Griffin, P.M., Slutsker, L., 1998. An outbreak of *Escherichia coli* O157:H7 infections associated with leaf lettuce consumption. J. Infect. Dis. 177, 1588–1593. https://doi.org/10.1086/515323.

Anjali, Kumar, S., Korra, T., Thakur, R., Arutselvan, R., Kashyap, A.S., Nehela, Y., Chaplygin, V., Minkina, T., Keswani, C., 2023. Role of plant secondary metabolites in defence and transcriptional regulation in response to biotic stress. Plant Stress 8, 100154. https://doi.org/10.1016/j.stress.2023.100154.

Bae, J.-Y., Seo, Y.-H., Oh, S.-W., 2022. Antibacterial activities of polyphenols against foodborne pathogens and their application as antibacterial agents. Food Sci. Biotechnol. 31, 985–997. https://doi.org/10.1007/s10068-022-01058-3.

Baker, C.J., Kovalskaya, N.Y., Mock, N.M., Deahl, K.L., Whitaker, B.D., Roberts, D.P., Hammond, R.W., Aver'yanov, A.A., 2013. Real-time monitoring of the extracellular redox potential of cell suspensions during plant/bacterial interactions. Physiol. Mol. Plant Pathol. 82, 20–27. https://doi.org/10.1016/j.pmpp.2013.01.002.

Baker, C.J., Mock, N.M., Smith, J.M., Aver'Yanov, A.A., 2015. The dynamics of apoplast phenolics in tobacco leaves following inoculation with bacteria. Front. Plant Sci. 6. https://doi.org/10.3389/fpls.2015.00649.

Baker, C.J., Mock, N.M., Whitaker, B.D., Hammond, R.W., Nemchinov, L., Roberts, D.P., Aver'yanov, A.A., 2014. Characterization of apoplast phenolics: *in vitro* oxidation of acetosyringone results in a rapid and prolonged increase in the redox potential. Physiol. Mol. Plant Pathol. 86, 57–63. https://doi.org/10.1016/j.pmpp.2014.03.004.

Borges, A., Ferreira, C., Saavedra, M.J., Simões, M., 2013. Antibacterial activity and mode of action of ferulic and gallic acids against pathogenic bacteria. Microb. Drug Resist. 19, 256–265. https://doi.org/10.1089/mdr.2012.0244.

Brandl, M.T., Amundson, R., 2008. Leaf age as a risk factor in contamination of lettuce with *Escherichia coli* O157:H7 and *Salmonella enterica*. Appl. Environ. Microbiol. 74, 2298–2306. https://doi.org/10.1128/AEM.02459-07.

Chen, J.C., Patel, K., Smith, P.A., Vidyaprakash, E., Snyder, C., Tagg, K.A., Webb, H.E., Schroeder, M.N., Katz, L.S., Rowe, L.A., Howard, D., Griswold, T., Lindsey, R.L., Carleton, H.A., 2023. Reoccurring *Escherichia coli* O157:H7 strain linked to leafy greens–associated outbreaks, 2016–2019. Emerg. Infect. Dis. 29. https://doi.org/10.3201/eid2909.230069.

Cho, E., Gurdon, C., Zhao, R., Peng, H., Poulev, A., Raskin, I., Simko, I., 2023. Phytochemical and agronomic characterization of high-flavonoid lettuce lines grown under field conditions. Plants 12, 3467. https://doi.org/10.3390/plants12193467.

Ding, Q., Gu, G., Luo, Y., Nou, X., Micallef, S.A., 2025. Transcriptomic response of *Escherichia coli* O157:H7 on romaine lettuce from harvest to storage during the preprocessing interval. Postharvest Biol. Technol. 227, 113594. https://doi.org/10.1016/j.postharvbio.2025.113594.

Ding, Q., Gu, G., Nou, X., Micallef, S.A., 2024. Cultivar was more influential than bacterial strain and other experimental factors in recovery of *Escherichia coli* O157:H7 populations from inoculated live romaine lettuce plants. Microbiol. Spectr. 12, e03767. https://doi.org/10.1128/spectrum.03767-23.

Dragišić Maksimović, J., Maksimović, V., Živanović, B., Hadži-Tašković Šukalović, V., Vuletić, M., 2008. Peroxidase activity and phenolic compounds content in maize root and leaf apoplast, and their association with growth. Plant Sci. 175, 656–662. https://doi.org/10.1016/j.plantsci.2008.06.015.

FDA, O.I.R., 2022. Outbreak investigation of *Salmonella* typhimurium: brightfarms packaged Salad greens (July 2021). https://www.fda.gov/food/outbreaks-foodborne-illness/outbreak-investigation-salmonella-typhimurium-brightfarms-packaged-salad-greens-july-2021.

Ferelli, A.M.C., Bolten, S., Szczesny, B., Micallef, S.A., 2020. *Salmonella enterica* elicits and is restricted by nitric oxide and reactive oxygen species on tomato. Front. Microbiol. 11, 391. https://doi.org/10.3389/fmicb.2020.00391.

Garcia, A.V., Charrier, A., Schikora, A., Bigeard, J., Pateyron, S., De Tauzia-Moreau, M.-L., Evrard, A., Mithöfer, A., Martin-Magniette, M.L., Virlogeux-Payant, I., Hirt, H., 2014. *Salmonella enterica* Flagellin is recognized via FLS2 and activates PAMP-Triggered immunity in *Arabidopsis thaliana*. Mol. Plant 7, 657–674. https://doi.org/10.1093/mp/sst145.

George, A.S., Brandl, M.T., 2021. Plant bioactive compounds as an intrinsic and sustainable tool to enhance the microbial safety of crops. Microorganisms 9, 2485. https://doi.org/10.3390/microorganisms9122485.

Goudeau, D.M., Parker, C.T., Zhou, Y., Sela, S., Kroupitski, Y., Brandl, M.T., 2013. The *Salmonella* transcriptome in lettuce and cilantro soft rot reveals a niche overlap with the animal host intestine. Appl. Environ. Microbiol. 79, 250–262. https://doi.org/10.1128/AEM.02290-12.

Han, S., Ferelli, A.M.C., Lin, S.-S., Micallef, S.A., 2020. Stress response, amino acid biosynthesis and pathogenesis genes expressed in *Salmonella enterica* colonizing tomato shoot and root surfaces. Heliyon 6, e04952. https://doi.org/10.1016/j.heliyon.2020.e04952.

Hudson, C.L., Micallef, S.A., 2024. Epiphytic, attached, and internal *Escherichia coli* O157 : H7 subpopulations associating with romaine lettuce are strain-dependent and affected by relative humidity and Pre- and postharvest plant state. J. Food Saf. 44, e13169. https://doi.org/10.1111/jfs.13169.

Hutzler, P., Fischbach, R., Heller, W., Jungblut, T.P., Reuber, S., Schmitz, R., Veit, M., Weissenbock, G., Schnitzler, J.-P., 1998. Tissue localization of phenolic compounds in plants by confocal laser scanning microscopy. J. Exp. Bot. 49, 953–965. https://doi.org/10.1093/jxb/49.323.953.

Jacob, C., Melotto, M., 2020. Human pathogen colonization of lettuce dependent upon plant genotype and defense response activation. Front. Plant Sci. 10, 1769. https://doi.org/10.3389/fpls.2019.01769.

Ji, M., Li, C., Li, Q., 2015. Rapid separation and identification of phenolics in crude red grape skin extracts by high performance liquid chromatography coupled to diode array detection and tandem mass spectrometry. J. Chromatogr. A 1414, 138–146. https://doi.org/10.1016/j.chroma.2015.08.041.

Kim, D.-E., Shang, X., Assefa, A.D., Keum, Y.-S., Saini, R.K., 2018. Metabolite profiling of green, Green/Red, and red lettuce cultivars: variation in health beneficial compounds and antioxidant potential. Food Res. Int. 105, 361–370. https://doi.org/10.1016/j.foodres.2017.11.028.

Lee, J.-S., Chandra, D., Son, J., 2022. Growth, physicochemical, nutritional, and postharvest qualities of leaf lettuce (*Lactuca sativa* L.) as affected by cultivar and amount of applied nutrient solution. Horticulturae 8, 436. https://doi.org/10.3390/horticulturae8050436.

Lester, G.E., Lewers, K.S., Medina, M.B., Saftner, R.A., 2012. Comparative analysis of strawberry total phenolics via fast blue BB vs. folin–ciocalteu: assay interference by ascorbic acid. J. Food Compos. Anal. 27, 102–107. https://doi.org/10.1016/j.jfca.2012.05.003.

Liu, X., Li, Y., Micallef, S.A., 2023. Natural variation and drought-induced differences in metabolite profiles of red oak-leaf and romaine lettuce play a role in modulating the interaction with *Salmonella enterica*. Int. J. Food Microbiol. 385, 109998. https://doi.org/10.1016/j.ijfoodmicro.2022.109998.

Liu, X., Li, Y., Micallef, S.A., 2022. Developmentally related and drought-induced shifts in the kale metabolome limited *Salmonella enterica* association, providing novel insights to enhance food safety. Food Microbiol. 108, 104113. https://doi.org/10.1016/j.fm.2022.104113.

Machado-Moreira, B., Richards, K., Brennan, F., Abram, F., Burgess, C.M., 2019. Microbial contamination of fresh produce: what, where, and how? Compr. Rev. Food Sci. Food Saf. 18, 1727–1750. https://doi.org/10.1111/1541-4337.12487.

Melotto, M., Panchal, S., Roy, D., 2014. Plant innate immunity against human bacterial pathogens. Front. Microbiol. 5. https://doi.org/10.3389/fmicb.2014.00411.

Meng, F., Altier, C., Martin, G.B., 2013. *Salmonella* colonization activates the plant immune system and benefits from association with plant pathogenic bacteria. Environ. Microbiol. 15, 2418–2430. https://doi.org/10.1111/1462-2920.12113.

Nguyen, T.L.A., Bhattacharya, D., 2022. Antimicrobial activity of quercetin: an approach to its mechanistic principle. Molecules 27, 2494. https://doi.org/10.3390/molecules27082494.

Oblessuc, P.R., Matiolli, C.C., Melotto, M., 2020. Novel molecular components involved in callose-mediated arabidopsis defense against *Salmonella enterica* and *Escherichia coli* O157:H7. BMC Plant Biol. 20, 16. https://doi.org/10.1186/s12870-019-2232-x.

O'Brien, J.A., Daudi, A., Finch, P., Butt, V.S., Whitelegge, J.P., Souda, P., Ausubel, F.M., Bolwell, G.P., 2012. A peroxidase-dependent apoplastic oxidative burst in cultured arabidopsis cells functions in MAMP-elicited defense. Plant Physiology 158, 2013–2027. https://doi.org/10.1104/pp.111.190140.

Otify, A.M., ElBanna, S.A., Eltanany, B.M., Pont, L., Benavente, F., Ibrahim, R.M., 2023. A comprehensive analytical framework integrating liquid chromatography-tandem mass spectrometry metabolomics with chemometrics for metabolite profiling of lettuce varieties and discovery of antibacterial agents. Food Res. Int. 172, 113178. https://doi.org/10.1016/j.foodres.2023.113178.

Podgórska, A., Burian, M., Szal, B., 2017. Extra-cellular but extra-ordinarily important for cells: apoplastic reactive oxygen species metabolism. Front. Plant Sci. 8, 1353. https://doi.org/10.3389/fpls.2017.01353.

Qi, J., Wang, J., Gong, Z., Zhou, J.-M., 2017. Apoplastic ROS signaling in plant immunity. Curr. Opin. Plant Biol. 38, 92–100. https://doi.org/10.1016/j.pbi.2017.04.022.

Rangel, J.M., Sparling, P.H., Crowe, C., Griffin, P.M., Swerdlow, D.L., 2005. Epidemiology of *Escherichia coli* O157:H7 outbreaks, United States. https://doi.org/10.3201/eid1104.040739.

Rickman, J.C., Barrett, D.M., Bruhn, C.M., 2007. Nutritional comparison of fresh, frozen and canned fruits and vegetables. Part 1. Vitamins C and B and phenolic compounds. J. Sci. Food Agric. 87, 930–944. https://doi.org/10.1002/jsfa.2825.

Roy, D., Melotto, M., 2019. Stomatal response and human pathogen persistence in leafy greens under preharvest and postharvest environmental conditions. Postharvest Biol. Technol. 148, 76–82. https://doi.org/10.1016/j.postharvbio.2018.10.013.

Roy, D., Panchal, S., Rosa, B.A., Melotto, M., 2013. *Escherichia coli* O157:H7 induces stronger plant immunity than *Salmonella enterica* typhimurium SL1344. Phytopathology 103, 326–332. https://doi.org/10.1094/PHYTO-09-12-0230-FI.

Shao, D., Li, Jing, Li, Ji, Tang, R., Liu, L., Shi, J., Huang, Q., Yang, H., 2015. Inhibition of gallic acid on the growth and biofilm formation of *Escherichia coli* and *Streptococcus mutans*. J. Food Sci. 80, M1299–M1305. https://doi.org/10.1111/1750-3841.12902.

Shi, C., Liu, H., 2021. How plants protect themselves from Ultraviolet-B radiation stress. Plant Physiology 187, 1096–1103. https://doi.org/10.1093/plphys/kiab245.

Shirron, N., Yaron, S., 2011. Active suppression of early immune response in tobacco by the human pathogen *Salmonella* typhimurium. PLoS One 6, e18855. https://doi.org/10.1371/journal.pone.0018855.

Shraim, A.M., Ahmed, T.A., Rahman, M.M., Hijji, Y.M., 2021. Determination of total flavonoid content by aluminum chloride assay: a critical evaluation. LWT 150, 111932. https://doi.org/10.1016/j.lwt.2021.111932.

Simmonds, M.S.J., 2003. Flavonoid–insect interactions: recent advances in our knowledge. Phytochemistry 64, 21–30. https://doi.org/10.1016/S0031-9422(03)00293-0.

Stearns, R., Freshour, A., Shen, C., 2022. Literature review for applying peroxyacetic acid And/or hydrogen peroxide to control foodborne pathogens on food products. J. Agric. Food Res. 10, 100442. https://doi.org/10.1016/j.jafr.2022.100442.

Sun, Z., Zhang, X., Wu, H., Wang, H., Bian, H., Zhu, Y., Xu, W., Liu, F., Wang, D., Fu, L., 2020. Antibacterial activity and action mode of chlorogenic acid against *salmonella* enteritidis, a foodborne pathogen in chilled fresh chicken. World J. Microbiol. Biotechnol. 36, 24. https://doi.org/10.1007/s11274-020-2799-2.

Taniguchi, M., LaRocca, C.A., Bernat, J.D., Lindsey, J.S., 2023. Digital database of absorption Spectra of diverse flavonoids enables structural comparisons and quantitative evaluations. J. Nat. Prod. 86, 1087–1119. https://doi.org/10.1021/acs.jnatprod.2c00720.

Torres, M.A., Jones, J.D.G., Dangl, J.L., 2006. Reactive oxygen species signaling in response to pathogens. Plant Physiology 141, 373–378. https://doi.org/10.1104/pp.106.079467.

U.S. Food and Drug Administration, 2020. Factors Potentially Contributing to the Contamination of Romaine Lettuce Implicated in the Three Outbreaks of *E. coli* O157:H7 During the Fall of 2019 (Investigation Report).

Wang, L., Chen, M., Lam, P.-Y., Dini-Andreote, F., Dai, L., Wei, Z., 2022. Multifaceted roles of flavonoids mediating plant-microbe interactions. Microbiome 10, 233. https://doi.org/10.1186/s40168-022-01420-x.

Wang, S., Yao, J., Zhou, B., Yang, J., Chaudry, M.T., Wang, M., Xiao, F., Li, Y., Yin, W., 2018. Bacteriostatic effect of quercetin as an antibiotic alternative *in vivo* and its antibacterial mechanism *In vitro*. J. Food Protect. 81, 68–78. https://doi.org/10.4315/0362-028X.JFP-17-214.

Zhao, J., Dixon, R.A., 2010. The 'Ins' and 'Outs' of flavonoid transport. Trends Plant Sci. 15, 72–80. https://doi.org/10.1016/j.tplants.2009.11.006.